Investigation of Thermal Effects in Structural Health Monitoring using Piezoelectric Sensors for Aerospace Applications

By

Bilal Hussain

(Registration No: 00000328719)

Supervised By

Dr. Anas bin Aqeel

Department of Mechatronics Engineering

College of Electrical & Mechanical Engineering

National University of Sciences & Technology (NUST)

Islamabad, Pakistan

(2024)

THESIS ACCEPTANCE CERTIFICATE

Certified that final copy of MS/MPhil thesis by NS Bilal Hussain. Registration No. 00000328719, of Electrical and Mechanical Engineering College has been vetted by undersigned, found complete in all respects as per NUST Statues/Regulations, is free of plagiarism, errors, and mistakes and is accepted as partial fulfillment for award of MS/MPhil degree. It is further certified that necessary amendments as pointed out by GEC members of the scholar have also been incorporated in the said thesis.
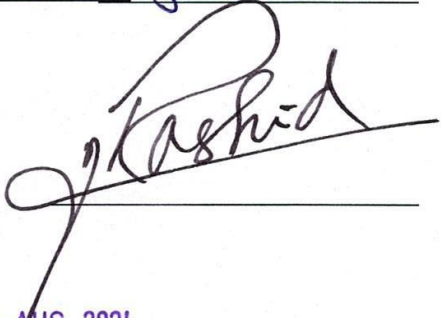
Signature: _____

Name of Supervisor: __Dr Anas Bin Aqeel__

Dated: _____16 Aug 2024_____

Signature of HOD: _____

Dr. Hamid Jabbar

Date: _____16 Aug 2024_____

Signature of Dean _____

Brig Dr Nasir Rashid

Date: _____16 AUG 2024_____

DEDICATION

I would like to dedicate this to my Parents and Siblings whose wonderful and amazing support led me here to this remarkable achievement.

ACKNOWLEDGEMENTS

ABSTRACT

A Structural Health Monitoring (SHM) system can continuously report on the structure's status, perform data analysis, and deliver assessment results automatically. SHM systems can play a very important role, especially in aerospace structures in which a variety of low-weight materials i.e. when composites are in use, where it is very necessary to know the health and degradation level of such structures. To measure the health of such structures using SHM systems various sensors/transducers are required. Piezoelectric sensors have been is used in SHM systems for the past few decades because of their many advantages such as robustness, fast response time, compact size, and versatility. A few active and passive technologies have been developed to make use of piezoelectric sensors for example Guided waves (GW), Acoustic emission and Electromechanical Impedance (EMI). The piezoelectric sensors have a vast variety of advantages but they are also prone to some disadvantages during their usage. These disadvantages mostly occur due to certain environmental effects like temperature, radiation, and vibration etc. Environmental effects and damages to the structure play a significant role on the data acquisition by the sensors. In this paper, we are trying to measure the effect of structural damage and temperature on the sensors used to collect the data for an EMI-based SHM system and develop a technique using various Machine Learning Algorithms to compensate for these effects.

Keywords: Structural Health Monitoring (SHM), Electromechanical Impedance (EMI), Carbon Fiber, Machine Learning,

TABLE OF CONTENTS

LIST OF TABLES

LIST OF FIGURES

Page No.

CHAPTER 1 STRUCTURAL HEALTH MONITORING

1.1 Introduction:

Structural Health Monitoring (SHM) is a crucial field dedicated to keeping track of and preserving the condition of structures over time. It uses various technologies to continuously check, assess, and manage the state of structural components to ensure they are safe and performing well. SHM's goals include spotting damage, understanding its seriousness, predicting how long the structure will last, and improving maintenance to avoid problems. The system usually involves sensors that measure things like strain, movement, and vibrations, along with data collection tools and analysis methods to interpret the information and guide decisions. SHM techniques range from simple visual inspections to more advanced methods like acoustic emission [1] , vibration monitoring [2], ultrasonic testing [3], and fiber optic sensing [4]. Each method has its strengths for detecting and analyzing issues. However, SHM also faces challenges such as handling large amounts of data, dealing with environmental effects on sensor accuracy, and managing the costs and complexity of implementing these systems. The field is advancing with new sensor technologies, better data analysis methods, and integration with emerging technologies like the Internet of Things (IoT) [5] and artificial intelligence [6], which are expected to improve how effectively SHM systems ensure the safety and durability of structures.

1.2 Advantages of Structural Health Monitoring:

Structural Health Monitoring (SHM) offers several key advantages that contribute to the safety, reliability, and longevity of structures. Here are the primary benefits of SHM, supported by references from various journal papers and research studies:

1.2.1   *Early Detection of Damage*

SHM systems enable the early detection of damage or deterioration in structures. By identifying issues at an early stage, SHM helps prevent minor problems from escalating into major failures. This proactive approach improves safety and reduces repair costs. For example, a study by Boller et al, [7] highlights that SHM systems can detect damage early, allowing for timely intervention and maintenance.

1.2.2   Enhanced Safety

Continuous monitoring of structures ensures that any changes in their condition are detected promptly, which enhances the overall safety of the structure. This is particularly important for critical infrastructure such as bridges and buildings. According to Cawley and Adams [8], SHM contributes significantly to maintaining safety by providing real-time data on the structural integrity

1.2.3   Cost-Effective Maintenance

SHM helps optimize maintenance schedules by providing accurate information about the condition of structures. This targeted approach allows for maintenance to be carried out only when necessary, thus saving costs compared to routine or reactive maintenance strategies. Farrar et al, [9] emphasizes that SHM can lead to significant cost savings by focusing maintenance efforts on areas that truly need attention.

1.2.4   Extended Structural Lifespan

By monitoring structural health continuously, SHM can help extend the lifespan of a structure. Early detection of issues and timely repairs can prevent major damage and deterioration, ultimately prolonging the life of the structure. Inman et al, [10] discuss how SHM contributes to extending the service life of structures by facilitating timely repairs and maintenance.

1.2.5   Improved Design and Construction Practices

Data collected from SHM systems can be used to improve future design and construction practices. Understanding how structures perform in real-world conditions provides valuable insights that can be applied to enhance the design and construction of new structures. This application of SHM data is noted in the work of Rytter [11], who highlight how SHM data helps refine engineering practices.

1.2.6   Reduced Downtime

SHM systems can help minimize downtime by allowing for predictive maintenance and repairs. This is crucial for infrastructure that is critical to daily operations, such as transportation systems and industrial facilities. A study by Sohn et al, [12] points out that SHM facilitates predictive maintenance, reducing the need for unexpected shutdowns and operational disruptions.

1.2.7 Enhanced Data for Decision-Making

SHM provides detailed and accurate data about the condition of a structure, which supports informed decision-making regarding repairs, upgrades, and resource allocation. This data-driven approach improves the management of structural assets. As noted by Worden et al. [13], the availability of comprehensive data allows for better decision-making and resource management.

1.2.8 Integration with Modern Technologies

SHM systems are increasingly integrated with modern technologies such as the Internet of Things (IoT) and artificial intelligence (AI), which enhances their capabilities and effectiveness. These technologies enable real-time monitoring, advanced data analysis, and automated decision-making. Zhang et al. [14] discuss how IoT and AI integration improves the functionality and efficiency of SHM systems.

1.3 Environmental Effects on Structural Health Monitoring (SHM)

Structural Health Monitoring (SHM) systems are crucial for ensuring the safety and longevity of infrastructure, but their effectiveness can be significantly influenced by environmental factors. Understanding these effects is essential for accurate data interpretation and reliable system performance. Below is a detailed overview of how various environmental conditions impact SHM, supported by relevant references.

1.3.1 Temperature Variations

Temperature changes can affect both the structural materials and the sensors used in SHM systems. Temperature fluctuations may cause thermal expansion or contraction of materials, leading to variations in sensor readings and structural responses. For instance, the impedance of piezoelectric sensors used in electromechanical impedance (EMI) techniques can vary with

temperature, impacting damage detection accuracy (Suresh and Ramesh, [15] Zhao et al. [16] note that temperature effects on sensor accuracy must be carefully managed to avoid false positives or negatives in damage detection

1.3.2   *Humidity and Moisture*

Humidity and moisture can impact the performance of sensors and the structural materials themselves. For example, moisture infiltration can affect the electrical properties of sensors and cause deterioration of structural materials. Studies such as those by Grosse et al. [17] highlight that moisture can lead to changes in the mechanical properties of materials, which in turn affects the accuracy of SHM systems Grosse, C.U, et al [18]. Additionally, changes in humidity can lead to sensor drift, affecting the reliability of the data collected

1.3.3   *Vibration and Dynamic Loads*

Dynamic loads and vibrations from traffic, wind, or seismic activity can influence the measurements taken by SHM systems. These environmental factors can cause noise or interference in sensor data, making it challenging to distinguish between structural responses due to damage and those due to external loads. Research by Farrar and Worden [9] emphasizes the need for advanced signal processing techniques to separate structural responses from dynamic loads

1.3.4   *Corrosion and Chemical Exposure*

Exposure to corrosive environments or chemicals can affect the integrity of both the structure and the SHM sensors. Corrosion can lead to material degradation, affecting the structural response and sensor accuracy. Additionally, chemicals can cause sensor components to degrade or malfunction. Research by Carper and K. [19] discusses the impact of corrosion on structural components and the implications for SHM systems

1.3.5   *Temperature and Humidity Cycles*

The combined effects of temperature and humidity cycles can exacerbate the challenges posed by each factor. Repeated cycles of temperature and humidity changes can lead to cumulative effects on both the sensors and the structural materials, potentially causing long-term performance issues.

1.4   Types of Sensors used in SHM

Structural Health Monitoring (SHM) relies on a variety of sensors to monitor the condition of structures like bridges, buildings, and tunnels. The latest advancements in SHM technology have expanded the types and applications of these sensors, improving the accuracy and reliability of monitoring systems. Some different types of sensors according to Machado, M. A et al [20] are;

1.4.1   *Strain Sensors:*

These sensors measure the deformation of materials under stress, making them crucial for monitoring load-bearing structures such as bridges and buildings. They detect tension, compression, bending, and torsion, offering precise data on structural integrity

1.4.2   *Crack Detection Sensors:*

These sensors are used to monitor cracks in concrete structures. They measure the position and length of cracks, which is vital for detecting early signs of structural failure.

1.4.3   *Vibration Sensors:*

Vibration sensors are critical for detecting changes in a structure's vibration patterns, which can indicate potential issues such as fatigue or the need for maintenance. They measure the g-force experienced by a structure, providing data on its dynamic response.

1.4.5   *Tilt Sensors (Inclinometers):*

These sensors monitor the inclination of structures, such as embankments and retaining walls. They help detect any tilting or movement that could lead to instability.

1.4.6   *Piezometers:*

Used primarily in geotechnical applications, piezometers monitor fluid pressures within soil and rock, which is essential for assessing the stability of embankments, dams, and other earth structures.

1.4.7 Fibre Optic Sensors (FOS):

These are widely used in SHM for real-time, continuous monitoring. FOS can measure strain, temperature, and even acoustic emissions, offering high sensitivity and durability.

1.4.8 Piezoelectric Sensors:

These sensors are commonly used for detecting vibrations, strain, and pressure changes. They are known for their ability to generate electrical signals in response to mechanical stress, making them highly effective in SHM applications.

1.4.9 Embedded Sensors:

These are integrated directly into materials during the manufacturing process. They provide continuous monitoring without compromising structural integrity. Innovations in smart materials and sensor systems are pushing the boundaries of what embedded sensors can achieve.

1.5 Piezoelectric Sensors in SHM

Piezoelectric sensors are widely used in Structural Health Monitoring (SHM) due to their high sensitivity, lightweight design, and ability to convert mechanical stress into electrical signals. These sensors are essential for detecting damage, monitoring strain, and evaluating the integrity of structures in real-time.

Recent advancements have focused on improving the performance of piezoelectric sensors through innovative materials and configurations. For instance, research has explored the use of piezo-ceramics and piezo-polymers in various SHM applications, such as damage detection in composite materials, localization of cracks in metallic structures, and even monitoring under extreme conditions like high temperatures [21], [22]

A review of state-of-the-art piezoelectric-based sensing techniques highlights the diversity of methods employed, including electromechanical impedance and ultrasonic Lamb waves. These techniques are crucial for developing next-generation self-powered and self-monitoring SHM systems, which are expected to enhance the efficiency and accuracy of monitoring large-scale infrastructure [23]

Piezoelectric sensors in Structural Health Monitoring (SHM) utilize various monitoring techniques to detect and analyze structural conditions. These techniques are diverse, each offering unique capabilities depending on the type of structural issue being monitored. Here are the main types of piezoelectric sensor monitoring techniques used in SHM;

1.5.1   Electromechanical Impedance Technique (EMI)

The EMI technique involves measuring the electrical impedance of piezoelectric sensors bonded to the structure. Variations in impedance indicate changes in structural properties, such as stiffness or the presence of damage [24] [25]

1.5.2   Ultrasonic Guided Wave Technique

This technique uses piezoelectric sensors to generate and receive guided ultrasonic waves that propagate through the structure. Changes in wave propagation, such as scattering or mode conversion, indicate the presence of damage like cracks or delamination [26] [27]

1.5.3   Acoustic Emission (AE) Technique

Piezoelectric sensors detect high-frequency elastic waves generated by the sudden release of energy from a structural source (e.g., crack growth or fiber breakage). The AE technique is sensitive to early-stage damage and can monitor dynamic events in real-time

1.5.4   Lamb Wave Method

Lamb waves are a type of guided wave used in SHM to detect damage in thin-walled structures. Piezoelectric sensors generate and capture these waves, and any changes in their propagation, such as time-of-flight or amplitude, are indicative of damage. [28] [29]

1.6   The Environmental Effects on Electromechanical Impedance-Based SHM

The Electromechanical Impedance (EMI) technique is a prominent method used in SHM for detecting structural damage. By leveraging the sensitivity of piezoelectric sensors to changes in structural impedance, this technique provides an effective means for early damage detection. However, like any SHM technique, the EMI method faces several challenges that can affect its accuracy, reliability, and practical implementation. Below is an exploration of these challenges faced while using EMI-based SHM.

1.6.1   Temperature Sensitivity

The impedance of piezoelectric sensors is highly sensitive to temperature variations. Temperature changes can lead to significant fluctuations in impedance readings, potentially leading to false positives or negatives in damage detection. Several approaches have been proposed to mitigate the effects of temperature. Bhalla and Soh [30]suggest the use of temperature compensation algorithms that adjust impedance measurements based on temperature readings from the environment. Advanced modeling techniques that incorporate temperature effects into the damage detection algorithm have also been developed.

1.6.2   Complex Signal Processing

The EMI technique requires complex signal processing to accurately interpret impedance data and distinguish between noise and actual structural damage. This complexity can limit the practical application of the technique, especially in real-time monitoring. Advances in machine learning and deep learning have been proposed to enhance the signal processing capabilities of EMI-based SHM. These techniques can help in automating the detection and classification of damage patterns, improving accuracy and reducing the computational load [31]

1.6.3   Sensor Bonding Issues

The effectiveness of the EMI technique heavily depends on the proper bonding of piezoelectric sensors to the structure. Poor bonding can lead to inconsistent impedance measurements and unreliable damage detection. To address bonding issues, researchers have developed guidelines for optimal sensor placement and bonding materials. Moreover, periodic

inspection and maintenance of sensor bonding are recommended to ensure long-term reliability [32]

1.6.4   *Limited Applicability to Complex Structures*

The EMI technique has limitations when applied to complex structures with multiple interacting components. The presence of multiple interfaces and boundaries can complicate the interpretation of impedance data, leading to potential inaccuracies in damage detection. Hybrid SHM approaches that combine EMI with other techniques, such as guided wave testing or acoustic emission, have been proposed to improve accuracy in complex structures. Additionally, advanced finite element modeling can be used to better understand the interactions between different components and improve data interpretation. [33].

1.6.5   *Power Supply Issues*

Continuous monitoring with the EMI technique requires a stable power supply, which can be challenging in remote or inaccessible locations. Researchers are exploring energy harvesting technologies that can power piezoelectric sensors using ambient energy sources, such as vibrations or solar power. This approach can help in sustaining long-term monitoring without the need for frequent battery replacements. [34]

This thesis is organized as follows: Chapter II provides an overview of past trends, current advancements, and future developments in the field of EMI-based SHM. Chapter III outlines the methodology used for experimenting and the data acquisition from the experiment. Chapter IV details filtration techniques applied to the data and the feature extraction techniques employed in this study. In Chapter V, the complete architecture of the machine learning algorithms used for classifying feature vectors is explained. Chapter VI presents the results, and Chapter VII concludes the study with final insights.

1.7 Summary

This chapter describes the basic introduction of SHM, its various advantages, limitations, and the key sensor technologies used. Furthermore, an introduction to the piezoelectric-based SHM system along with the multiple techniques that can be utilized in an SHM system are briefly

explained. Lastly an explanation of EMI-based SHM and some of the problems arising due to the environmental effects while using an EMI-based SHM along with their current solutions are given.

CHAPTER 2 LITERATURE REVIEW

2.1 Recent History of Structural Health Monitoring System

Park et al, (2000) proposed an integrated methodology for detecting and locating structural damage by combining two approaches. The first method utilizes piezoelectric materials to monitor changes in electrical impedance caused by shifts in the structure's mechanical impedance, allowing for qualitative damage detection. The second method employed a model-based wave propagation technique to quantitatively assess damage using frequency response function (FRF) data. High-frequency structural excitation through piezoelectric sensors was used to detect damage. Numerical and experimental results demonstrated the effectiveness of the technique. [32]

Park et al, (2001) explored the use of an impedance-based health monitoring technique for assessing critical civil infrastructure, such as pipelines, especially in urgent situations like post-earthquake evaluations. The method involved applying high-frequency excitations (above 30 kHz) via piezoelectric sensors to detect changes in structural impedance, indicating damage. The study demonstrated the technique's effectiveness in real-time damage detection and monitoring the integrity of structures both under normal conditions and after natural disasters. The results highlighted the method's capability for quick and reliable damage assessment. [35]

Chin-Wee et al, (2002) proposed an electro-mechanical (EM) impedance method that was initially explored for in-situ stress monitoring in structural health applications. A theoretical model based on Euler-Bernoulli beam theory was developed to analyze how in-situ stress influences the dynamic and EM responses of a smart beam with piezoceramic (PZT) transducers. Numerical simulations revealed that natural frequency shifts due to axial loads were not directly reflected in the EM admittance signature. This discrepancy led to the use of a genetic algorithm (GA) for accurately back-calculating the in-situ stress, addressing the challenge of interpreting EMI data. [36]

Kiong et al, (2003) presented a method for damage diagnosis using changes in mechanical impedance at high frequencies, measured through electro-mechanical impedance

(EMI) with piezoelectric-ceramic (PZT) patches. The approach incorporated both real and imaginary components of the admittance signature to quantify damage, eliminating the need for prior structural models. A complex damage metric was developed based on parameters like stiffness, mass, and damping. The methodology outperformed traditional low-frequency vibration and raw-signature-based damage quantification methods, as demonstrated in tests on a reinforced concrete frame subjected to base vibrations. [37]

Kiong et al, (2004) addressed the shear lag effect in the electromechanical impedance (EMI) technique for structural health monitoring (SHM), which was often overlooked in existing models. It examined how the adhesive bond layer between piezoelectric-ceramic (PZT) patches and structures affected force transfer and impedance measurements. The study integrated the shear lag effect into one-dimensional and two-dimensional impedance models and conducted a parametric analysis. Results indicated that the bond layer can significantly alter the electromechanical admittance response, highlighting the need for careful installation of PZT patches. [38]

Tseng et al, (2005) introduced an impedance-based method for identifying damage in thin plates using piezoelectric ceramic (PZT) transducers and a two-dimensional electromechanical impedance model. A damage identification scheme based on nonlinear optimization matched numerical and experimental electric admittance changes to locate and quantify damage. The method was validated through numerical simulations. [39]

Voutetaki et al, (2006) proposed a numerical method for structural health monitoring and damage identification in civil infrastructure using piezoelectric ceramic (PZT) patches. By comparing frequency-dependent electromechanical admittance signatures with baseline measurements, the health status of structures is assessed. Damage is quantified using the root-mean-square deviation (RMSD) index and further refined through statistical confidence methods in a computer software. Numerical simulations on concrete beams demonstrated the advantages of this mathematical modeling approach over traditional methods, which often lacked the accuracy needed for complex structures. [40]

Yang et al, (2007) presented an electromechanical impedance (EMI) model for monitoring the health of cylindrical shell structures using piezoceramic (PZT) transducers. A two-

dimensional impedance modeling approach was employed to obtain the admittance of PZT transducers. At the same time, the p-Ritz method was used to calculate the mechanical impedance of the cylindrical shell. Experimental tests on an aluminum cylindrical shell validated the developed EMI model by comparing theoretical and measured PZT admittance signatures in undamaged and damaged conditions. The feasibility of the EMI method for damage detection in cylindrical shell structures was also explored. [41]

Park et al, (2008) reported advancements in structural health monitoring (SHM) using electro-mechanical impedance sensors for damage diagnosis in civil, mechanical, and aerospace structures. The technique leveraged high-frequency excitations and piezoelectric sensors to detect changes in structural impedance, indicating potential damage. A novel impedance model was proposed for sensor self-diagnosis, along with a temperature-resistant damage detection algorithm based on frequency shifts and cross-correlation coefficients. Additionally, the paper introduced an active sensor node with integrated wireless sensing, data compression, and RF telemetry capabilities, enhancing local data processing for SHM applications. [42]

Rizzo et al, (2009) conducted EMI-based experiments on steel, aluminum, and concrete specimens to monitor load, crack development, and curing across various frequency ranges. A statistical index was used to evaluate the sensitivity of different frequency bands, and a novel signature gradient was applied to characterize signatures at each frequency. The findings demonstrated that optimizing frequency bands can streamline data acquisition, making the EMI technique more efficient for real-world applications. [43]

Rosiek et al (2010) investigated uncertainty and sensitivity analysis in Finite Element simulations for electro-mechanical impedance-based structural health monitoring. It evaluated how impedance measurements track damage by analyzing a beam with a bonded transducer through both deterministic and stochastic simulations. Key parameters influencing damage indexes were identified, and the effectiveness and robustness of the SHM system were discussed. [44]

Visalakshi et al, (2011) presented a sensor for detecting corrosion in bare steel rebars using electro-mechanical impedance (EMI) to identify changes in stiffness, mass, and

damping through shifts in conductance and susceptance signatures. Experiments with piezoelectric ceramic (PZT) sensors and induced corrosion show that EMI effectively detected and quantified corrosion. The findings, compared with ACM field machine data, highlight EMI's capability for early corrosion detection and measurement. [45]

Inman et al, (2012) presented an affordable, versatile measurement system for structural health monitoring (SHM) using electromechanical impedance (EMI), featuring real-time data acquisition and temperature compensation. It offered simpler implementation and lower cost compared to conventional impedance analyzers. Experiments on aluminum beams and plates with PZT patches validated the system's efficiency and effectiveness for real-time SHM. [46]

Siebel et al, (2013) studied the sensitivity of electromechanical impedance to structural damage under varying temperatures, using cross-correlation coefficients to compensate for temperature effects. Experiments were conducted on a carbon fiber reinforced plastic (CFRP) panel with 26 piezoelectric transducers of different sizes, subjected to temperatures ranging from -50°C to 100°C. The study assessed the impact of temperature on impedance measurements and evaluated the effectiveness of the temperature compensation approach. Additionally, it examined the sensitivity to impact damage and the influence of transducer size and location, concluding with a discussion on balancing sensing area and temperature range for reliable damage detection. [47]

Baptista et al, (2014) presented an experimental study examining how temperature impacts the electrical impedance of 5H PZT ceramic sensors commonly used in EMI. Results revealed that temperature effects are significantly frequency-dependent, highlighting a critical area for future research in SHM. [48]

Memmolo et al, (2016) explored various probabilistic reconstruction methods and signal transformation techniques to enhance impact damage detection using a sparse sensor array, particularly for aircraft structures. Simulations indicated that while single methods provided quick flaw detection, a combination of multiple analyses and reconstruction techniques offered more detailed insights into damage location and severity, provided that diagnostic parameters were thoroughly addressed. [49]

Giurgiutiu et al, (2016) examined the impact of radiation, temperature, and vacuum (RTV) on piezoelectric wafer active sensors (PWASs) for extending structural health monitoring (SHM) to aerospace applications. The research combined theoretical and experimental approaches using electromechanical impedance spectroscopy (EMIS). Theoretical models derived analytical expressions for the temperature sensitivity of EMIS resonance and anti-resonance, while experimental tests exposed PWAS transducers to RTV conditions and various temperatures. Results showed that RTV exposure caused less than 1% change in resonance frequencies but about 15% in amplitudes. Temperature sensitivity analyses indicated specific changes in resonance and anti-resonance parameters, with consistent trends across different PWAS transducers, leading to conclusions and suggestions for future research. [50]

Emmanuel et al, (2016) explored two temperature compensation methods for Structural Health Monitoring using piezoceramic transducers (PZT). One method applied linear regression to the PZT's static capacity from electromechanical impedance, while the other used Modes Frequency Shift (MFS) from frequency response functions. Experiments on a composite plate with five PZT patches showed that both methods effectively detect ±2°C temperature variations and could replace traditional temperature sensors. [51]

Alamdari et al, (2017) detailed a large-scale Structural Health Monitoring application on the Sydney Harbour Bridge, focusing on 800 jack arches under traffic lane 7. To identify potential structural damages or instrumentation issues, they proposed a novel non-model-based method using Spectral Moments (SMs) from measured responses. This method employs a modified k-means clustering algorithm to detect jack arches with abnormal responses. Evaluation with real bridge data successfully identified known issues and detected anomalies over a month of monitoring, which were confirmed as system issues. [52]

Oliveira et al, (2018) introduced a novel SHM approach combining electromechanical impedance (EMI)-PZT with CNNs, where EMI signatures are segmented and analyzed using Euclidean distances to create RGB frames. The method, tested on three PZTs bonded to an aluminum plate, achieved a 100% hit rate in pattern classification with minimal dataset requirements, demonstrating significant potential for industrial SHM applications. [53]

Antunes et al, (2019) presented a novel approach to mitigate temperature-induced errors in EMI-based SHM for pipelines, incorporating temperature compensation and finite element modeling of bonded piezoceramics. Experimental validation demonstrated the method's effectiveness, with successful temperature compensation across a wide range and accurate damage detection [54]

Valder et al, (2020) presented a novel approach to structural health monitoring (SHM) by integrating convolutional neural networks (CNN) with the electromechanical impedance (EMI) method. The study addressed the challenge of environmental influences, such as temperature variations, which can affect impedance-based damage detection. Using aluminum beams subjected to different temperatures, a one-dimensional CNN was trained to predict damage while compensating for temperature effects. This approach demonstrated improved accuracy in damage detection by accounting for environmental conditions. [55]

Khodaei et al, (2020) presented a structural health monitoring (SHM) methodology for detecting damage in composite bonded repairs using guided wave techniques. A two-step algorithm calculated and compared path damage indices (PDIs) to thresholds for reliable detection while reducing false alarms. A self-diagnosis approach using electromechanical impedance (EMI) identified faulty sensors, and a novel probability imaging technique based on Voronoi Tessellation localizes damage. Experimental results validated the method under varying operational and environmental conditions [56]

Gayakwad et al, (2022) This study introduced smart sensing units (SSU) composed of a PZT patch, adhesive, and steel plate, embedded in concrete to enhance damage detection. Combining EMI and wave propagation (WP) techniques improved the sensitivity of SSUs to detect both near-field and far-field damage. Numerical simulations and experimental validation demonstrated the effectiveness of this approach in monitoring structural changes in concrete. [57]

George et al, (2024) proposed a new approach using a 1-D convolutional neural network to identify cracks in fiber-reinforced concrete through raw electromechanical impedance (EMI) signatures from piezoelectric (PZT) transducers. Experimental results showed the method's effectiveness, achieving 95.24% accuracy and demonstrating reliable damage identification in a

PZT-enabled SHM system. The leave-one-specimen-out cross-validation ensures realistic validation. [58]

2.2 Summary

This chapter provides a comprehensive review of the recent developments, current advancements, and future directions of structural health monitoring (SHM) systems, with a particular focus on electromechanical impedance (EMI)-based techniques. The extensive body of research on EMI-based SHM is thoroughly discussed, highlighting studies that have explored innovative applications and methods to address challenges associated with the existing systems. This detailed analysis aims to contribute to the ongoing efforts in improving EMI-based SHM, ultimately paving the way for enhanced accuracy and reliability in structural damage detection.

CHAPTER 3 EXPERIMENTAL METHADOLOGY

3.1 Experimental Setup:

A series of experiments were performed on an aerospace material to investigate the EMI resulting from varying degrees of induced damage at various temperatures. The specimen utilized in these experiments consisted of a beam of Carbon Fiber Figure 1 (Uncracked), with dimensions of 150mm x 40mm x 0.5mm each. Two PZT5 piezoelectric sensors with a diameter of 18mm and thickness of 0.23mm were used as both an actuator and a sensor. The sensing PZT5 sensor was positioned 15mm from one edge of the specimen, while the actuating sensor was placed 10 mm from the other edge, with a distance of 80 mm between them. The PZT patches were attached to the specimen using Depoxy steel.

Figure 1 Carbon Fiber Specimen

The specimen under observation were subjected to varying levels of damage during experiments. The damage was induced as cracks located 75mm from one edge of the total 150mm length of the specimen. The cracks were of varying lengths, ranging from 10mm Figure 2 (a), 20mm Figure 2(b) and 40mm (Full Cracked) Figure 2(c). Lastly,a reference specimen with no cracks (Uncracked) was added as the reference for the induced EMI.
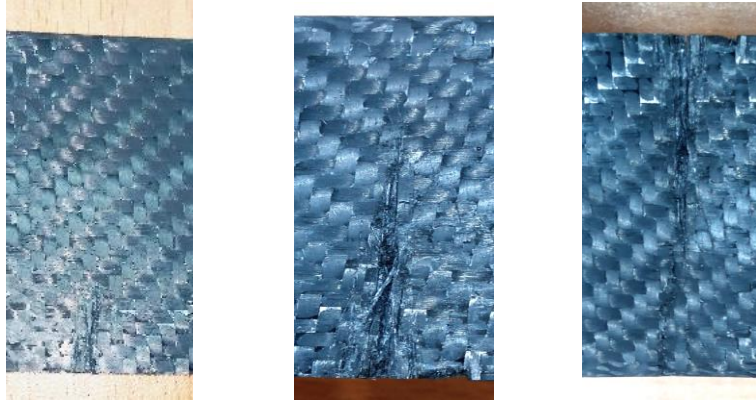
Figure 2 (a) Quarter Cracked (b) Half Cracked (c) Full Cracked

The specimen was positioned inside an insulated Acrylic chamber Figure 3 with the dimensions of 12 inches (height) x 12 inches (length) x 11.25 inches (width). The purpose of the insulated Acrylic chamber was to maintain a controlled temperature environment and to avoid interference from external conditions during experiments. A heating coil was employed to elevate the temperature inside the chamber, with the temperature range extending from 30°C to 60°C, with 5°C increments. The ambient temperature inside the chamber was monitored using a thermocouple sensor that was positioned slightly above the specimens. The thermocouple had a sensing range from -20°C to 80°C. The temperature was constantly monitored using a UNO Arduino controller.

Figure 3 Insulated Acrylic Chamber

Figure 4 LCR Meter and Power Supply

The Electromechanical impedance was measured using a Matrix LCR meter MCR-6200A (Figure 4), having an operational frequency range of 12Hz to 200 KHz. The data acquisition from the LCR meter was done using Labview software on a Personal Computer Figure 5 (A TITAN DC Power Supply (Figure 4) was utilized to supply the voltage to the actuator.
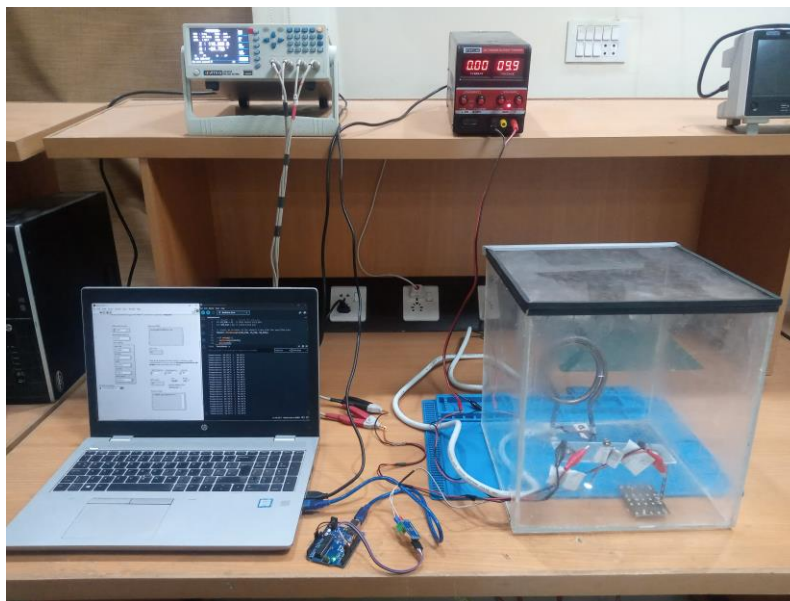

Figure 5 Complete Experimental setup including LCR Meter, Power Supply, Personal Computer, and the Insulated Acrylic Chamber

3.2 Experimental Results:

The experimental results obtained can be described in two ways. Firstly the electromechanical impedance obtained as a result of various kinds of damage on the material. Secondly, the electromechanical impedance was obtained as a result of the temperature change.

3.2.1 Damage Effect

The figure presents Electromechanical Impedance (EMI) results obtained from experiments conducted on uncracked and fully-cracked Carbon Fiber beams. The Real Part (Figure 6) Imaginary Part (Figure 7), and Magnitude (Figure 8) of the impedance were measured for both conditions. The data reveals that damage to the material does not significantly affect the Imaginary Part or the Magnitude of the impedance. However, the Real Part of the impedance shows a notable difference at the resonant frequency of 4 kHz. Specifically, the peak impedance for the undamaged Carbon Fiber is approximately 750 Ω, whereas for the fully-cracked Carbon Fiber, the peak impedance decreases to about 600 Ω. Additionally, it was observed that at frequencies above 10 kHz, the change in impedance becomes negligible, indicating that low-frequency ranges are more sensitive and thus more suitable for detecting damage in Carbon Fiber materials.
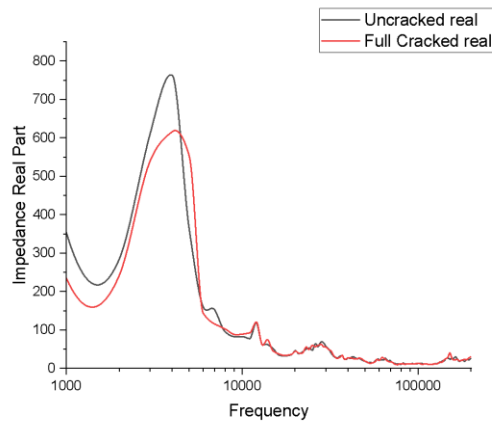

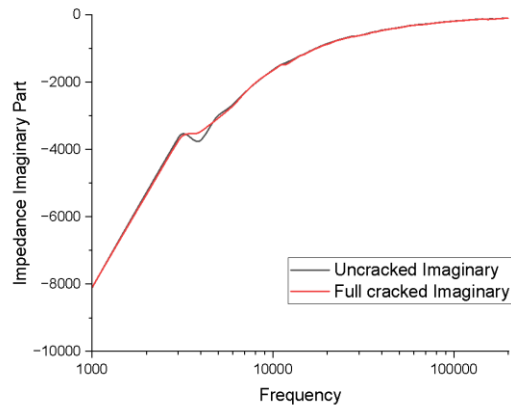Figure 6 Real Part of Impedance of UC and FC Carbon Fiber

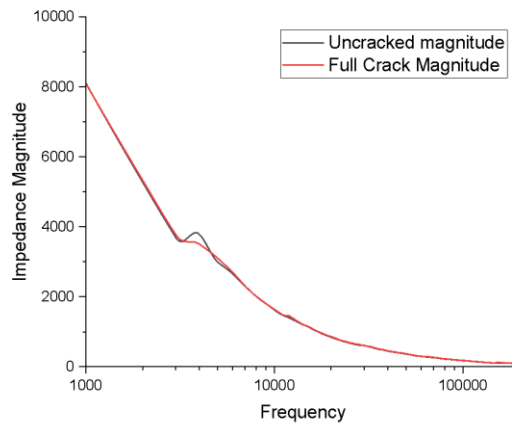Figure 7 Imaginary part of Impedance of UC and FC Carbon Fiber

Figure 8 Magnitude of Impedance of UC and FC Carbon Fiber

3.2.2   *Temperature effect:*

The Electromechanical Impedance (EMI) results obtained from an un-cracked Carbon Fiber specimen subjected to varying temperatures are shown in the figures below. Unlike the effect of structural damage, temperature variations cause slight differences in the Imaginary Part (Figure 10) and Magnitude (Figure 11) of the impedance. However, these changes remain negligible when compared to the more pronounced changes observed in the Real Part of the impedance (Figure 9). Specifically, at a resonant frequency, the Real impedance decreases significantly from approximately 750 Ω at 30°C to about 450 Ω at 60°C. This finding highlights

the sensitivity of the Real Part of the impedance to temperature variations, making it a critical parameter for monitoring temperature effects in Structural Health Monitoring systems.
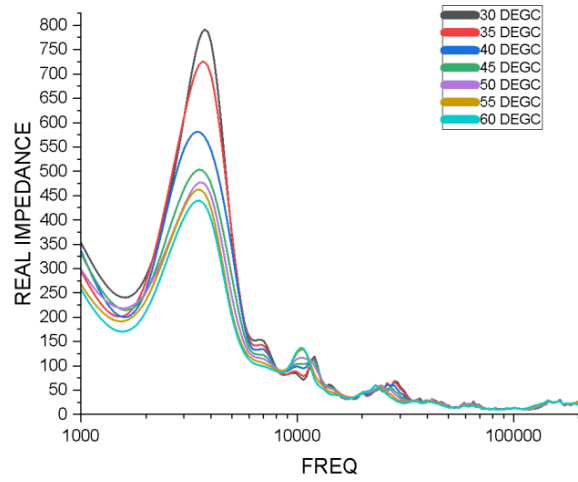

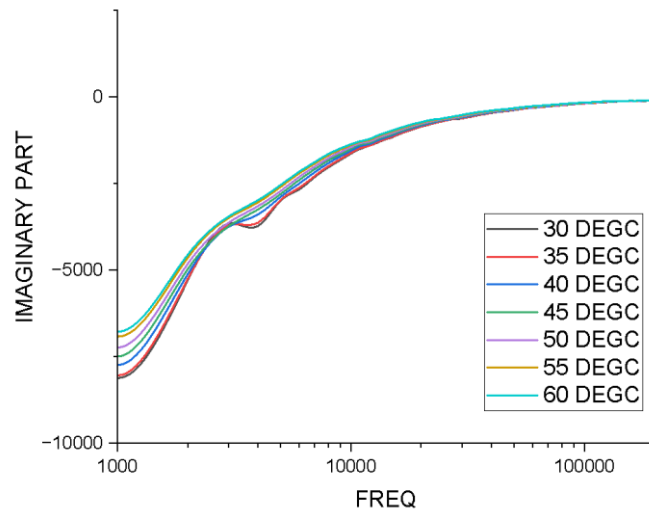Figure 9 Real Part of Impedance of UC Carbon Fiber at Different Temperatures.

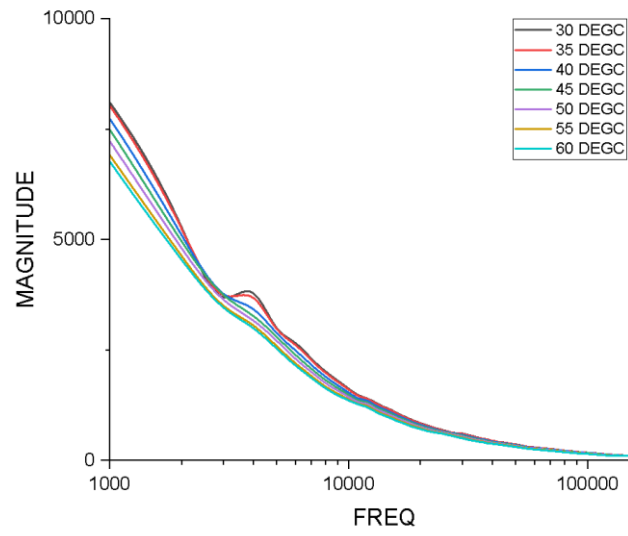Figure 10 Imaginary Part of Impedance of UC Carbon Fiber at Different Temperatures

Figure 11 Magnitude of Impedance of UC Carbon Fiber at Different Temperatures

CHAPTER 4 DAMAGE DETECTION THROUGH MACHINE LEARNING:

To develop a robust method for detecting damage under varying thermal conditions, we employed machine-learning techniques that require the impedance data derived from experimental results. The dataset, comprises of impedance measurements recorded at multiple temperatures, was systematically analyzed to classify damage into four distinct categories: UC (Un-Cracked), QC (Quarter-Cracked), HC (Half-Cracked), and FC (Fully Cracked).

Dataset Overview:

- **Classes:** UC, QC, HC, FC
- **Temperature Range:** Seven discrete temperature values (30°C, 35°C, 40°C, 45°C, 50°C, 55°C, 60°C)
- **Impedance Measurements:** For each temperature, impedance data were collected at 199 frequency points spanning from 1 kHz to 199 kHz, with a 1 kHz interval between each measurement point

To detect damage using machine learning, we utilized the data obtained and applied the following steps;

4.1 Data Filtration:

Data filtration, or data filtering, is a process used to remove, modify, or retain specific data points or certain frequencies from a dataset. These frequencies may involve the removal of noise or any other irrelevant piece of information not required for our purpose. In our case, it involves the removal of data at frequencies higher than 10 KHz. This is the data that cannot be utilized and hence may act as noise during the process of Machine Learning.

A low-pass filter was utilized to obtain the data below the desired frequency range of 10 KHz. The filter was applied to the raw data obtained from the four different cases i.e. un-cracked (UC), quarter-cracked (QC), half-cracked (HC), and fully-cracked (FC). The data was

filtered using the Matlab® 'Filter Designer' app to design a low pass filter with a 0-10 KHz passband frequency. Figure 12 shows the raw data from un-cracked piece of carbon fiber. Whereas Figure 13 shows the acquired data after filtration.
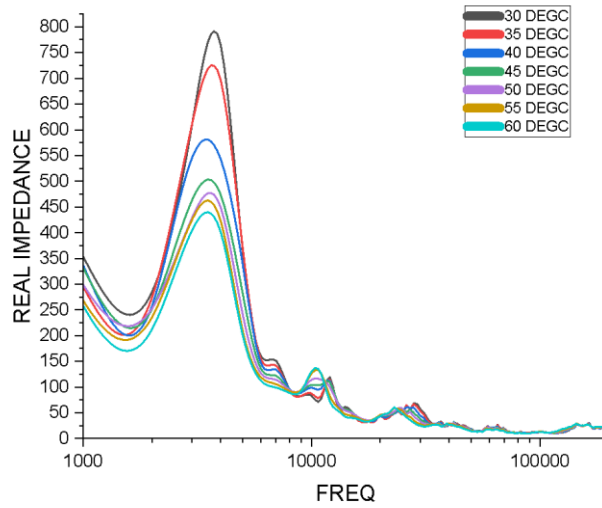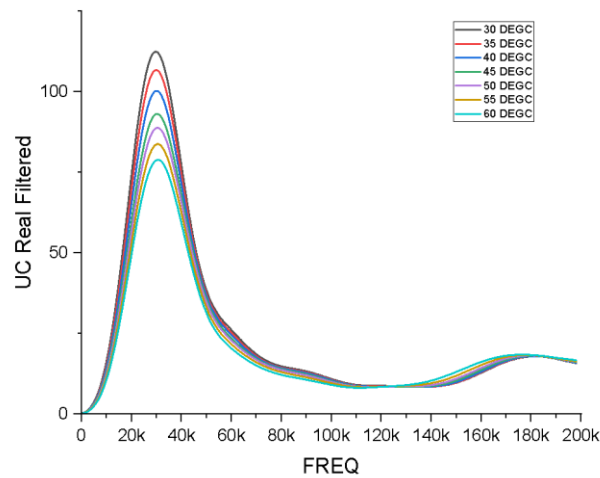

Figure 12 Un-Filtered UC Data

Figure 13 Filtered Un-cracked Data

4.2 Feature Extraction

Three distinct features—average band power, peak, and mean—were extracted from the filtered data using MATLAB® functions 'bandpower', 'peak', and 'mean', respectively. These features provide critical insights into the underlying data, enhancing the robustness and

26

accuracy of the classification process. Additionally, Independent Component Analysis (ICA) was performed on the filtered data, and the resulting components were utilized as an extracted feature for classification. To emphasize the significance of feature extraction, the filtered data itself was also included as a feature during classification. This approach highlights the comparative effectiveness of using derived features versus raw filtered data in improving classification outcomes.

CHAPTER 5 CLASSIFICATION ALGORITHMS

Weka® tool has been utilized to classify the extracted features and the filtered data. The Classifiers used are;

5.1 Linear discriminant analysis (LDA)

Linear Discriminant Analysis (LDA) is a classification and dimensionality reduction technique that aims to project data onto a lower-dimensional space while maximizing class separability. It does this by finding the linear combinations of features that best distinguish between classes, assuming that the data for each class is normally distributed and that the classes share the same covariance matrix. LDA works by calculating the within-class and between-class scatter matrices, then solving an eigenvalue problem to determine the optimal projection directions. It is widely used in applications where linear boundaries are effective for classifying data. The LDA was implemented using the WEKA® software. The results are shown in Table 1 Performance of Different Feature Vectors in LDA.

Table 1 Performance of Different Feature Vectors in LDA

Linear discriminant analysis (LDA)		
Feature Vector	Confusion Matrix	%age Accuracy
Average Band Power	$\begin{array}{cccc} a & b & c & d \\ \begin{bmatrix} 58 & 8 & 18 & 15 \\ 31 & 38 & 15 & 15 \\ 27 & 11 & 41 & 20 \\ 26 & 14 & 12 & 47 \end{bmatrix} \end{array}$ a = UC ,b =QC, c= HF, d= FC	46.4646 %
Mean	$\begin{array}{cccc} a & b & c & d \\ \begin{bmatrix} 59 & 5 & 33 & 2 \\ 19 & 61 & 3 & 16 \\ 7 & 18 & 58 & 16 \\ 19 & 9 & 22 & 49 \end{bmatrix} \end{array}$	57.3232 %

	a = UC ,b =QC, c= HF, d= FC	
Peak	a b c d $$\begin{bmatrix} 59 & 5 & 32 & 3 \\ 19 & 62 & 3 & 15 \\ 8 & 17 & 59 & 15 \\ 17 & 10 & 22 & 50 \end{bmatrix}$$ a = UC ,b =QC, c= HF, d= FC	58.0808 %
Filtered Raw Data	a b c d $$\begin{bmatrix} 99 & 36 & 50 & 14 \\ 67 & 80 & 17 & 35 \\ 58 & 55 & 63 & 23 \\ 23 & 26 & 51 & 99 \end{bmatrix}$$ a = UC ,b =QC, c= HF, d= FC	42.8392 %
Independent Component analysis (ICA)	a b c d $$\begin{bmatrix} 59 & 12 & 14 & 14 \\ 14 & 66 & 7 & 12 \\ 20 & 22 & 46 & 11 \\ 9 & 1 & 9 & 80 \end{bmatrix}$$ a = UC ,b =QC, c= HF, d= FC	63.3838 %

In Table 1 above the performance of various feature extraction techniques combined with Linear Discriminant Analysis (LDA) was evaluated using confusion matrices and accuracy metrics, the Independent Component Analysis (ICA) method exhibited the % classification accuracy at 63.38%, surpassing all other feature vectors. The Peak feature vector achieved an accuracy of 58.08%, followed by the Mean feature vector with 57.32% accuracy. The Average Band Power feature vector yielded an accuracy of 46.46%, while the Filtered Raw Data approach showed the lowest accuracy at 42.84%.

Table 2 Summary LDA Cross Validation

	Average Band Power	Mean	Peak	Filtered Raw Data	Independent Component Analysis (ICA)
Correctly Classified Instances	46.4646 %	57.3232 %	58.0808 %	42.8392 %	63.3838 %
Incorrectly Classified Instances	53.5354 %	42.6768 %	41.9192 %	57.1608 %	36.6162 %
Kappa statistic	0.2862	0.431	0.4411	0.2379	0.5118
Mean absolute error	0.325	0.2901	0.2886	0.3404	0.2873
Root mean squared error	0.3979	0.3725	0.3716	0.4087	0.3705
Relative absolute error	86.6586 %	77.3496 %	76.9556 %	90.7658 %	76.6136 %
Root relative squared error	91.8769 %	86.0178 %	85.8051	94.3922	85.5516 %

These results in Table 2 compare the performance of different feature vectors (Average Band Power, Mean, Peak, Filtered Raw Data, and Independent Component Analysis (ICA)) in a classification task by LDA. ICA has the highest classification accuracy (63.38%) and the best performance across several metrics, including Kappa statistic (0.5118) and the lowest relative errors. The Peak and Mean features also perform reasonably well, with classification

accuracies around 58% and similar Kappa statistics (~0.44), indicating moderate agreement. The filtered raw data performs the worst with only 42.84% classification accuracy and the highest errors, showing that more sophisticated feature extraction techniques, such as ICA, significantly improve classification accuracy and error rates.

5.2 Quadratic discriminant analysis (QDA):

Quadratic Discriminant Analysis (QDA) is a classification technique similar to Linear Discriminant Analysis (LDA) but relaxes the assumption that the covariance matrices of the classes are identical. Instead, QDA allows each class to have its own covariance matrix, which enables it to model more complex, non-linear decision boundaries between classes. This makes QDA more flexible than LDA, particularly for problems where the classes are not linearly separable. However, this flexibility comes at the cost of requiring more data to estimate the separate covariance matrices accurately. QDA is especially useful when there are significant differences in the variance of the features within each class. The results acquired through the use of Weka are shown below in Table 3.

Table 3 Performance of Different Feature Vectors in QDA

Quadratic discriminant analysis (QDA)		
Feature Vector	Confusion Matrix	%age Accuracy
Average Band Power	a b c d $$\begin{bmatrix} 94 & 0 & 5 & 0 \\ 9 & 66 & 24 & 0 \\ 6 & 1 & 92 & 0 \\ 9 & 0 & 7 & 83 \end{bmatrix}$$ a = UC ,b =QC, c= HF, d= FC	84.596 %
	a b c d $$\begin{bmatrix} 95 & 0 & 4 & 0 \\ 1 & 86 & 12 & 0 \\ 8 & 0 & 91 & 0 \\ 3 & 0 & 5 & 91 \end{bmatrix}$$ a = UC ,b =QC, c= HF, d= FC	

31

Mean		91.6667 %
Peak	$\begin{array}{cccc} a & b & c & d \end{array}$ $\begin{bmatrix} 95 & 0 & 4 & 0 \\ 2 & 85 & 12 & 0 \\ 9 & 0 & 90 & 0 \\ 3 & 0 & 5 & 91 \end{bmatrix}$ a = UC ,b =QC, c= HF, d= FC	91.1616 %
Filtered Raw Data	$\begin{array}{cccc} a & b & c & d \end{array}$ $\begin{bmatrix} 137 & 5 & 55 & 2 \\ 13 & 116 & 67 & 3 \\ 15 & 4 & 179 & 1 \\ 8 & 2 & 62 & 127 \end{bmatrix}$ a = UC ,b =QC, c= HF, d= FC	70.2261 %
Independent Component Analysis (ICA)	$\begin{array}{cccc} a & b & c & d \end{array}$ $\begin{bmatrix} 71 & 4 & 23 & 1 \\ 0 & 99 & 0 & 0 \\ 19 & 2 & 78 & 0 \\ 0 & 0 & 0 & 99 \end{bmatrix}$ a = UC ,b =QC, c= HF, d= FC	87.6263 %

In Table 3 above the performance of different feature vectors using Quadratic Discriminant Analysis (QDA) was assessed. The results, including confusion matrices and accuracy metrics, showed that the mean feature vector achieved the highest accuracy of 91.67%, closely followed by the peak feature vector, which had an accuracy of 91.16%. The Independent Component Analysis (ICA) method also demonstrated strong   achieved an accuracy of 84.60%, while the Filtered Raw Data approach yielded the lowest accuracy at 70.23%.

Table 4 Summary QDA Cross Validation

	Average Band Power	Mean	Peak	Filtered Raw Data	Independent Component Analysis (ICA)

	84.596 %	91.6667 %	91.1616 %	70.2261 %	87.6263 %
Correctly Classified Instances					
Incorrectly Classified Instances	15.404 %	8.3333 %	8.8384 %	29.7739 %	12.3737 %
Kappa statistic	0.7946	0.8889	0.8822	0.603	0.835
Mean absolute error	0.0955	0.0433	0.0428	0.1738	0.073
Root mean squared error	0.234	0.1683	0.1678	0.32	0.2091
Relative absolute error	25.4621 %	11.5448 %	11.4163 %	46.3447 %	19.4788 %
Root relative squared error	54.0487 %	38.8698 %	38.7571 %	73.9057 %	48.2962 %

Table 4 results demonstrate significantly improved classification performance across the various feature extraction methods. The **Mean** and **Peak** features achieve the highest classification accuracy (91.67% and 91.16%, respectively), with very low error metrics such as the Mean Absolute Error (0.0433 and 0.0428) and high Kappa statistics (0.8889 and 0.8822), indicating strong agreement and accuracy in classification. The **ICA** method also performs well with 87.63% correctly classified instances and a Kappa statistic of 0.835, indicating robust performance but slightly lower than Mean and Peak. The **Average Band Power** also shows strong classification at 84.60%, though the **Filtered Raw Data** method performs the worst with only 70.23% accuracy, higher error metrics, and the lowest Kappa statistic (0.603). This further emphasizes that advanced feature extraction techniques like ICA, Mean, and Peak provide better classification results compared to raw or basic filtered data.

5.3 Naïve Bayes (NB):

Naïve Bayes is a simple yet powerful probabilistic classification algorithm based on Bayes' Theorem, with the assumption that the features are conditionally independent given the class label. Despite this strong and often unrealistic assumption of independence, Naïve Bayes works surprisingly well in many practical applications, particularly in text classification, spam detection, and document categorization. It calculates the probability of each class based on the input features and assigns the class with the highest posterior probability. Naïve Bayes is fast, efficient, and works well with high-dimensional data, making it a popular choice for large datasets despite its simplicity. The results from Weka are shown in Table 5.

Table 5 Performance of Different Feature Vectors in Naïve Bayesian Classifier

Naïve Bayesian classifier (NB):		
Feature Vector	Confusion Matrix	%age Accuracy
Average Band Power	a b c d $\begin{bmatrix} 13 & 70 & 11 & 5 \\ 8 & 69 & 15 & 7 \\ 10 & 72 & 11 & 6 \\ 16 & 67 & 13 & 3 \end{bmatrix}$ a = UC ,b =QC, c= HF, d= FC	24.2424 %
Mean	a b c d $\begin{bmatrix} 11 & 57 & 22 & 9 \\ 8 & 52 & 29 & 10 \\ 12 & 59 & 22 & 6 \\ 18 & 53 & 25 & 3 \end{bmatrix}$ a = UC ,b =QC, c= HF, d= FC	22.2222 %
	a b c d	22.2222 %

34

Peak	$\begin{bmatrix} 12 & 58 & 22 & 7 \\ 8 & 51 & 30 & 10 \\ 14 & 58 & 22 & 5 \\ 18 & 52 & 26 & 3 \end{bmatrix}$ a = UC ,b =QC, c= HF, d= FC	
Filtered Raw Data	a b c d $\begin{bmatrix} 51 & 99 & 46 & 3 \\ 37 & 110 & 31 & 21 \\ 46 & 110 & 39 & 4 \\ 51 & 86 & 47 & 15 \end{bmatrix}$ a = UC ,b =QC, c= HF, d= FC	27.0101 %
Independent Component Analysis (ICA)	a b c d $\begin{bmatrix} 53 & 14 & 23 & 9 \\ 7 & 61 & 10 & 21 \\ 17 & 12 & 67 & 3 \\ 7 & 10 & 3 & 79 \end{bmatrix}$ a = UC ,b =QC, c= HF, d= FC	65.6566 %

Table 6 Summary Naïve Bayes Cross Validation

	Average Band Power	Mean	Peak	Filtered Raw Data	Independent Component Analysis (ICA)
Correctly Classified Instances	24.2424 %	22.2222 %	22.2222 %	27.0101 %	65.6566 %

Incorrectly Classified Instances	75.7576 %	77.7778 %	77.7778 %	72.9899 %	34.3434 %
Kappa statistic	-0.0101	-0.037	-0.037	0.0268	0.5421
Mean absolute error	0.3817	0.384	0.384	0.3739	0.2466
Root mean squared error	0.4584	0.4557	0.4557	0.4336	0.3456
Relative absolute error	101.7823 %	102.3886 %	102.3898 %	99.6954 %	65.7502 %
Root relative squared error	105.8688 %	105.2352 %	105.2335 %	100.1394 %	79.8129 %

Table 6 results reflect the performance of various feature extraction methods in a classification task using the Naïve Bayes classifier. The Independent Component Analysis (ICA) method performs best with 65.66% correctly classified instances and a Kappa statistic of 0.5421, indicating moderate agreement. This is significantly better than the other methods, which all have much lower accuracy (around 22-27%) and negative or near-zero Kappa statistics, indicating poor performance. The Mean Absolute Error **and** Root Mean Squared Error metrics are also lowest for ICA, while the other methods have higher errors and poor relative performance. This suggests that ICA is the most suitable feature extraction method for Naïve Bayes in this context, while the others fail to effectively capture the relationships in the data.

5.4 Support vector machine (SVM):

Support Vector Machine (SVM) is a powerful supervised learning algorithm used for classification and regression tasks. It works by finding the optimal hyperplane that maximally separates data points of different classes in a high-dimensional space. SVM uses support vectors,

which are the data points closest to the hyperplane, to define the boundary. The algorithm is particularly effective in handling both linear and non-linear classification problems by applying kernel functions (e.g., polynomial, radial basis function) to transform the input data into a higher-dimensional space where a linear separation is possible. SVM is known for its ability to perform well in complex, high-dimensional datasets and to generalize effectively to unseen data, making it widely used in various fields such as text categorization, image recognition, and bioinformatics. Weka results for SVM are shown in Table 7.

Table 7 Performance of Different Feature Vectors in Support Vector Machine

Support vector machine (SVM)		
Feature Vector	Confusion Matrix	%age Accuracy
e Average Band Power	$\begin{array}{cccc} a & b & c & d \end{array}$ $\begin{bmatrix} 88 & 4 & 3 & 4 \\ 8 & 84 & 3 & 4 \\ 6 & 5 & 68 & 20 \\ 24 & 4 & 10 & 61 \end{bmatrix}$ a = UC ,b =QC, c= HF, d= FC	76.0101 %
Mean	$\begin{array}{cccc} a & b & c & d \end{array}$ $\begin{bmatrix} 94 & 0 & 1 & 4 \\ 3 & 93 & 3 & 0 \\ 9 & 3 & 77 & 10 \\ 19 & 0 & 21 & 59 \end{bmatrix}$ a = UC ,b =QC, c= HF, d= FC	81.5657 %
Peak	$\begin{array}{cccc} a & b & c & d \end{array}$ $\begin{bmatrix} 85 & 1 & 4 & 9 \\ 3 & 92 & 3 & 1 \\ 8 & 2 & 79 & 10 \\ 17 & 0 & 20 & 62 \end{bmatrix}$ a = UC ,b =QC, c= HF, d= FC	80.303 %

	a b c d	
Filtered Raw Data	$\begin{bmatrix} 42 & 42 & 65 & 50 \\ 24 & 73 & 71 & 31 \\ 5 & 37 & 108 & 43 \\ 24 & 17 & 65 & 93 \end{bmatrix}$ a = UC ,b =QC, c= HF, d= FC	39.6985 %
Independent Component Analysis (ICA)	$\begin{bmatrix} 24 & 34 & 11 & 30 \\ 17 & 44 & 13 & 25 \\ 18 & 41 & 16 & 24 \\ 16 & 37 & 12 & 34 \end{bmatrix}$ a = UC ,b =QC, c= HF, d= FC	29.798 %

In Table 7 above, we evaluated the performance of a Support Vector Machine (SVM) classifier. The table shows that the Mean features achieved the highest classification accuracy at 81.57%, demonstrating superior performance in distinguishing between the classes. In contrast, the Filtered Raw Data and ICA features resulted in significantly lower accuracies of 39.70% and 29.80%, respectively, indicating these feature sets were less effective.

Table 8 Summary Support Vector Machine Cross Validation

	Average Band Power	Mean	Peak	Filtered Raw Data	Independent Component Analysis (ICA)
Correctly Classified Instances	76.0101 %	81.5657 %	80.303 %	39.6985 %	29.798 %
Incorrectly Classified Instances	23.9899 %	18.4343 %	19.697 %	60.3015 %	70.202 %

Kappa statistic	0.6801	0.7542	0.7374	0.196	0.064
Mean absolute error	0.1199	0.0922	0.0985	0.3015	0.351
Root mean squared error	0.3463	0.3036	0.3138	0.5491	0.5925
Relative absolute error	31.9856 %	24.5784 %	26.2619 %	80.4014 %	93.6001 %
Root relative squared error	79.9808 %	70.1109 %	72.4722 %	126.8076 %	136.819 %

The Table 8 results show the performance of various feature extracted when using a Support Vector Machine (SVM) classifier. The Mean and Peak features exhibit the best performance, with correctly classified instances of 81.57% and 80.30%, respectively, along with relatively high Kappa statistics of 0.7542 and 0.7374, indicating substantial agreement in classification. Average Band Power also performs well with 76.01% accuracy and a Kappa of 0.6801. In contrast, Filtered Raw Data and ICA have much lower classification accuracies, particularly ICA, which only classifies 29.80% of instances correctly and has the lowest Kappa statistic (0.064), indicating poor classification performance. This suggests that SVM performs well with certain feature extraction methods like Mean and Peak, while it struggles with raw data and ICA in this context.

5.5 Multi-Class Classifier (MCC)

A Multi-Class Classifier (MCC) is a classification algorithm designed to handle problems with more than two classes. Unlike binary classifiers, which deal with only two possible outcomes, MCC can classify instances into one of several categories. Common approaches to multi-class classification include methods such as **one-vs-one**, where a separate classifier is trained for each pair of classes, and **one-vs-rest**, where a classifier is trained for each class against all other classes combined. Popular algorithms like Support Vector Machines, Decision Trees, and Neural

Networks can be adapted for multi-class classification by using these strategies. MCCs are widely used in fields where data naturally belongs to multiple categories, such as image classification, natural language processing, and medical diagnosis. MCC results from WEKA are shown in Table 9

Table 9 Performance of Different Feature Vectors in Multi-Class Classifier

Multi-Class Classifier (MCC)		
Feature Vector	Confusion Matrix	%age Accuracy
Average Band Power	a b c d $\begin{bmatrix} 41 & 16 & 32 & 10 \\ 0 & 92 & 5 & 2 \\ 7 & 9 & 69 & 14 \\ 6 & 3 & 11 & 79 \end{bmatrix}$ a = UC ,b =QC, c= HF, d= FC	70.9596 %
Mean	a b c d $\begin{bmatrix} 43 & 17 & 30 & 9 \\ 0 & 92 & 3 & 4 \\ 14 & 11 & 62 & 12 \\ 6 & 3 & 11 & 79 \end{bmatrix}$ a = UC ,b =QC, c= HF, d= FC	69.697 %
Peak	a b c d $\begin{bmatrix} 44 & 16 & 31 & 8 \\ 0 & 94 & 2 & 3 \\ 11 & 11 & 64 & 13 \\ 7 & 3 & 10 & 79 \end{bmatrix}$ a = UC ,b =QC, c= HF, d= FC	70.9596 %
Filtered Raw Data	a b c d	

		50.7538 %
	$\begin{bmatrix} 80 & 41 & 60 & 18 \\ 4 & 144 & 13 & 38 \\ 31 & 58 & 77 & 33 \\ 24 & 23 & 49 & 103 \end{bmatrix}$ a = UC ,b =QC, c= HF, d= FC	
Independent Component Analysis (ICA)	a b c d $\begin{bmatrix} 61 & 9 & 14 & 15 \\ 14 & 66 & 7 & 12 \\ 22 & 22 & 46 & 9 \\ 9 & 1 & 8 & 81 \end{bmatrix}$ a = UC ,b =QC, c= HF, d= FC	64.1414 %

In Table 9 above, we evaluated the performance of a Multi-Class Classifier. The evaluation reveals that the Average Band Power and Peak feature sets provided the highest classification accuracy of 70.96%, indicating their effectiveness in distinguishing between classes. The Mean feature set followed closely with an accuracy of 69.70%. In contrast, the Filtered Raw Data and ICA features exhibited lower accuracies, with 50.75% and 64.14%,

Table 10 Summary Multi Class Classifier Cross Validation

	Average Band Power	Mean	Peak	Filtered Raw Data	Independent Component Analysis (ICA)
Correctly Classified Instances	70.9596 %	69.697 %	70.9596 %	50.7538 %	64.1414 %
Incorrectly Classified Instances	29.0404 %	30.303 %	29.0404 %	49.2462 %	35.8586 %

Kappa statistic	0.6128	0.596	0.6128	0.3434	0.5219
Mean absolute error	0.2165	0.2234	0.2219	0.3306	0.2973
Root mean squared error	0.3188	0.3229	0.3219	0.4045	0.3741
Relative absolute error	57.7229 %	59.5589 %	59.1786 %	88.1666 %	79.2647 %
Root relative squared error	73.6104 %	74.5795 %	74.3343 %	93.4147 %	86.3928 %

The Table 10 results compare the performance of different feature extraction methods using a **Multi-Class Classifier (MCC)**. **Average Band Power** and **Peak** both achieve the highest classification accuracy at **70.96%**, followed closely by **Mean** at **69.70%**, all with substantial Kappa statistics around **0.61**, indicating strong performance. **Independent Component Analysis (ICA)** also performs reasonably well with **64.14%** accuracy and a Kappa statistic of **0.5219**, though its errors are slightly higher. **Filtered Raw Data** shows the weakest performance, with only **50.75%** accuracy, a low Kappa of **0.3434**, and the highest error metrics. This indicates that while MCC can handle multi-class problems effectively, its performance heavily depends on the quality of the feature extraction method used, with Average Band Power, Peak, and ICA being more effective than raw data.

5.6 Random Forest (RF):

Random Forest (RF) is an ensemble learning algorithm widely used for classification and regression tasks. It operates by constructing multiple decision trees during training and combining their outputs to improve predictive accuracy and control overfitting. Each tree is trained on a random subset of the data, and features are randomly selected at each split in the trees, making the forest more diverse and robust. The final classification or regression result is

typically based on a majority vote from the individual trees. RF is highly effective in handling large datasets, including those with high dimensionality or missing data, and offers excellent performance across a wide range of applications such as image recognition, bioinformatics, and finance due to its strong generalization capabilities. The WEKA results for RF are shown in Table 11

Table 11 Performance of Different Feature Vectors in Random Forest Classifier

Random Forest (RF)		
Feature Vector	Confusion Matrix	%age Accuracy
Average Band Power	a b c d $\begin{bmatrix} 21 & 25 & 33 & 20 \\ 14 & 21 & 45 & 19 \\ 27 & 38 & 19 & 15 \\ 20 & 18 & 32 & 29 \end{bmatrix}$ a = UC ,b =QC, c= HF, d= FC	22.7273 %
Mean	a b c d $\begin{bmatrix} 20 & 22 & 32 & 25 \\ 14 & 23 & 45 & 17 \\ 27 & 39 & 18 & 15 \\ 26 & 18 & 27 & 28 \end{bmatrix}$ a = UC ,b =QC, c= HF, d= FC	22.4747 %
Peak	a b c d $\begin{bmatrix} 23 & 22 & 31 & 23 \\ 13 & 23 & 43 & 20 \\ 29 & 35 & 20 & 15 \\ 29 & 18 & 28 & 24 \end{bmatrix}$ a = UC ,b =QC, c= HF, d= FC	22.7273 %
	a b c d	

Filtered Raw Data	$\begin{bmatrix} 70 & 43 & 54 & 32 \\ 32 & 71 & 63 & 33 \\ 49 & 58 & 57 & 35 \\ 43 & 27 & 43 & 86 \end{bmatrix}$ a = UC ,b =QC, c= HF, d= FC	35.6784 %
Independent Component Analysis (ICA)	a b c d $\begin{bmatrix} 86 & 4 & 8 & 1 \\ 4 & 87 & 3 & 5 \\ 16 & 7 & 76 & 0 \\ 1 & 2 & 5 & 91 \end{bmatrix}$ a = UC ,b =QC, c= HF, d= FC	85.8586 %

In the Table 11**Error! Reference source not found.** above, we evaluated the performance of the Random Forest Classifier. The evaluation reveals that the Independent Component Analysis (ICA) feature set delivers the best performance with an accuracy of 85.86%, far surpassing other feature sets. Filtered Raw Data also shows relatively better performance with an accuracy of 35.68%. In contrast, the Average Band Power, Mean, and Peak feature sets exhibit notably lower accuracies, ranging from 22.47% to 22.73%, indicating that they are less effective for the Random Forest classifier in this context.

Table 12 Summary Random Forrest Cross Validation

	Average Band Power	Mean	Peak	Filtered Raw Data	Independent Component analysis (ICA)
Correctly Classified Instances	22.7273 %	22.4747 %	22.7273 %	35.6784 %	85.8586 %

	77.2727 %	77.5253 %	77.2727 %	64.3216 %	14.1414 %
Incorrectly Classified Instances	77.2727 %	77.5253 %	77.2727 %	64.3216 %	14.1414 %
Kappa statistic	-0.0303	-0.0337	-0.0303	0.1424	0.8114
Mean absolute error	0.3947	0.3954	0.3925	0.3427	0.1445
Root mean squared error	0.4968	0.4982	0.496	0.4428	0.243
Relative absolute error	105.2496 %	105.4482 %	104.6705 %	91.3796 %	38.5444 %
Root relative squared error	114.717 %	115.0563 %	114.717 %	102.2646 %	56.1174 %

These results in Table 12 show the performance of various feature extraction methods using the **Random Forest (RF) classifier**. **Independent Component Analysis (ICA)** stands out with the highest accuracy of **85.86%**, a substantial Kappa statistic of **0.8114**, and the lowest error metrics (e.g., Mean Absolute Error of **0.1445** and Root Mean Squared Error of **0.243**). This indicates excellent classification performance for ICA. In contrast, the **Average Band Power**, **Mean**, and **Peak** methods perform poorly, with accuracy around **22.7%**, negative Kappa statistics (indicating performance worse than random chance), and high error values. **Filtered Raw Data** performs better than these methods but still lags behind ICA, with **35.68%** accuracy and a low Kappa statistic of **0.1424**. These results emphasize that ICA is particularly well-suited for Random Forest, while other feature extraction methods struggle with this classifier.

CHAPTER 6 COMPARISON OF RESULTS

This chapter presents the classification accuracies obtained after the Machine Learning algorithms were implemented on the data. Five distinct features were analyzed using six different classifiers within the WEKA® software environment. From the above-mentioned tables in Chapter 5, it is clear that the accuracy while training the QDA Classifier along with the Mean value as a feature vector yields the highest accuracy. The results also indicate that classifiers capable of handling multi-class problems exhibit higher accuracy compared to those limited to binary or fewer class distinctions.

Table 13 shows the Average Classification Accuracy across the four Classes. Quadratic Discriminant Analysis (QDA) consistently outperforms other classifiers across most features, achieving the highest accuracy with the Mean and Peak features, at 91.67% and 91.16%, respectively. The Independent Component Analysis (ICA) feature also demonstrates strong performance, particularly with QDA (87.63%) highlighting its robustness in classification tasks. Conversely, the Naïve Bayesian classifier (NB) shows relatively low accuracy across most features, except ICA, where it performs significantly better (65.66%). Support Vector Machine (SVM) performs well with Average Band Power, Mean, and Peak, but poorly with ICA. The Multi-Class Classifier (MCC) and Random Forest (RF) show moderate performance, with MCC generally performing better than RF, except for ICA where RF excels. The overall performance of these classifiers suggests that feature selection is critical to optimizing classification accuracy, with ICA and QDA emerging as particularly effective combinations.

Table 13 Average Classification accuracy

Average Classification accuracy						
	Linear discriminant analysis (LDA)	Quadratic discriminant analysis (QDA)	Naïve Bayesian classifier (NB)	Support vector machine (SVM)	Multi-Class Classifier (MCC)	Random Forest (RF)

Average Band Power	46.46%	84.60%	24.24%	76.01%	70.96%	22.73%
Mean	57.32%	91.67%	22.22%	81.57%	69.70%	22.47%
Peak	58.08%	91.16%	22.22%	80.30%	70.96%	22.73%
Filtered Raw Data	42.84%	70.23%	27.01%	39.70%	50.75%	35.68%
Independent Component Analysis (ICA)	63.38%	87.63%	65.66%	29.80%	64.14%	85.86%

The bar chart (ccuracy of classification model

Table 14) displays the comparative performance of various features in classification tasks. The features evaluated include Average Band Power, Mean, Peak, and Filtered Raw Data, along with the application of Independent Component Analysis (ICA). Among these, ICA achieves the highest classification accuracy, approaching 70%, indicating its superior capability in distinguishing classes within the dataset. Peak and Mean features also show robust performance, with accuracy levels above 50%, suggesting that these features capture critical aspects of the data relevant to classification. The Filtered Raw Data, while still effective, results in the lowest accuracy, highlighting the importance of feature extraction and selection in improving classification outcomes. This analysis underscores the value of ICA and specific feature extractions in enhancing the accuracy of classification model

Table 14 Average Classification Accuracy of Different Features
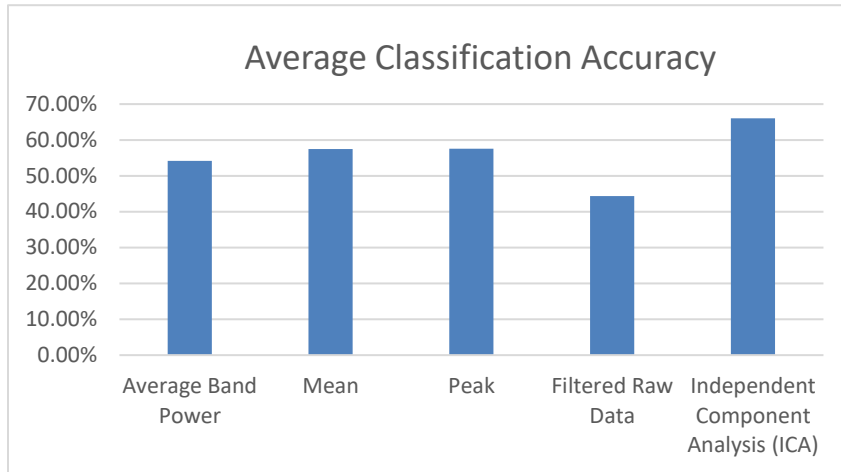
The bar chart (Table 15) provides the average performance of the classifiers: Linear Discriminant Analysis (LDA), Quadratic Discriminant Analysis (QDA), Naïve Bayesian (NB), Support Vector Machine (SVM), Multi-Class Classifier (MCC), and Random Forest (RF). The QDA and RF classifiers demonstrate superior performance, each achieving accuracy levels near 90%. This high accuracy suggests these classifiers are particularly effective in managing the dataset's complexities. Conversely, the SVM classifier records the lowest accuracy, highlighting its relative inefficacy. The results reinforce the observation that classifiers capable of handling multi-class problems, such as MCC, tend to perform better in terms of accuracy, confirming the importance of selecting an appropriate classifier based on problem complexity.

Table 15 Average Classification Accuracy of the Classifiers

Average Classification Accuracy
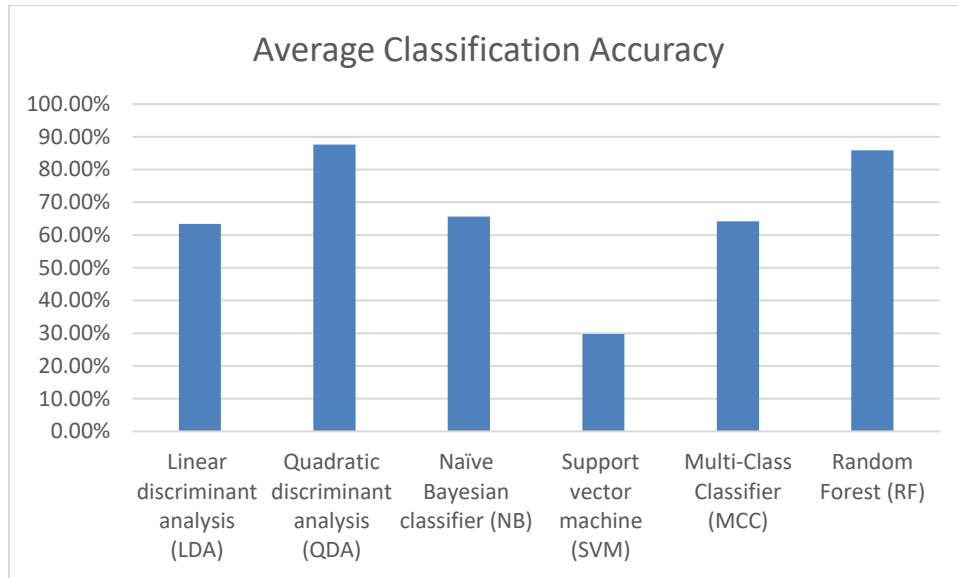
CHAPTER 7 SUMMARY & CONCLUSION:

This research presents a method for detecting varying levels of damage under different temperatures in Electromechanical Impedance (EMI)-based Structural Health Monitoring (SHM) systems. Experiments were conducted on Carbon Fiber specimen subjected to different temperature conditions and degrees of damage. To accurately detect and classify damage at various temperatures, Machine Learning (ML) algorithms were implemented, leveraging features extracted from the experimental data. The evaluation of different feature extraction methods—Filtered Raw Data, ICA, Mean, Peak, and Band Power—across classification models including LDA, QDA, Naïve Bayes, SVM, and Multi-Class Classifier, revealed that ICA consistently outperformed other methods, particularly within the LDA and Naïve Bayes models. This indicates that ICA is a robust method for uncovering underlying patterns in the data that are beneficial for these classifiers. Mean and Peak features also performed strongly, notably within QDA and SVM models, demonstrating their ability to capture critical signal information for effective classification. On the contrary, the Filtered Raw Data consistently yielded poor results across all classifiers, emphasizing the importance of proper feature extraction in achieving accurate predictions. Additionally, there was variability in how well different classifiers responded to specific feature vectors, with ICA excelling in Naïve Bayes but showing weaker performance in SVM, while Mean and Peak performed consistently well across most models. This highlights the critical need for selecting and tailoring feature extraction methods to the specific classifiers being used to maximize model performance.

The results indicated that certain classifiers, such as Quadratic Discriminant Analysis (QDA), which achieved an average accuracy of 87.63%, outperformed others. This superior performance is attributed to the algorithm's ability to effectively handle multi-class data, which was inherent in this study. In contrast, classifiers less suited for multi-class problems exhibited lower accuracy.

In conclusion, the findings demonstrate that ML algorithms can effectively be used for damage detection in SHM systems under varying thermal conditions. However, achieving higher accuracy may require larger datasets. Future research should focus on expanding the dataset

by conducting more experiments at each temperature, which would enable the application of deep learning techniques to further improve classification accuracy

CHAPTER 8 FUTURE RECOMMENDATION

For future work, it is recommended to explore advanced and hybrid feature extraction techniques that combine methods such as ICA with statistical or frequency domain features (e.g., Mean, Peak, Band Power) to further enhance classification accuracy. Additionally, testing more sophisticated classifiers such as deep learning models (e.g., convolutional neural networks) could provide insights into non-linear relationships that simpler models might overlook. Cross-validation techniques should also be employed to ensure the generalizability of results across different datasets.

It is also recommended to increase the amount of datasets at each given temperature value to improve the accuracy of machine learning classifiers. This is particularly important for deep learning algorithms, which require a large number of datasets to effectively learn complex patterns and relationships within the data. Expanding the dataset would enhance the model's ability to generalize across different temperature values, reducing the risk of overfitting and improving overall classification performance.

Finally, incorporating domain knowledge, such as task-specific or physiological insights, into feature selection may improve classification performance and increase model interpretability.

REFERENCES

[1] T. Morton, R. Harrington and J. Bjeletich, "Acoustic emissions of fatigue crack growth.," *Engineering Fracture Mechanics,* p. 691–697, 1973,.

[2] H. A. M. S. a. N. S. Ali Bastani, "Identification of temperature variation and vibration disturbance in impedance-based structural health monitoring using piezoelectric sensor array method," *Structural Health Monitoring.. doi:10.1177/1475921711427486,* vol. 11, no. 3, pp. 305-314, December 14, 2011.

[3] C. Maraveas and T. Bartzanas, " Sensors for structural health monitoring of agricultural structures.," *Sensors,* Vols. 21, , no. 314., 2021, .

[4] J. M. a. A. Asundi, "Structural health monitoring using a fiber optic polarimetric sensor and a fiber optic curvature sensor-static and dynamic test. . Struct. , ,," *Smart Materials and Structures,* vol. 10, no. 181, 2001.

[5] F. Di Nuzzo, D. Brunelli, T. Polonelli and L. Benini, " Structural health monitoring system with narrowband IoT and MEMS sensors. ,," *IEEE Sensors J.,* Vols. 21, , no. 16371–16380., 2021.

[6] D. Olson, " Data mining in business services.," *Service Business,* Vols. 1,, no. 3, p. 181–193., 2007.

[7] C. C. F.-K. &. F. Y. Boller, Encyclopedia of Structural Health Monitoring, John Wiley and Sons., 2009.

[8] P. &. A. R. Cawley, ""The use of Lamb waves for the detection of damage in thin plates.","" *Journal of Nondestructive Testing,* vol. 14, no. 4, pp. 222-236., (1988)..

[9] C. &. W. K. Farrar, "Structural Health Monitoring: A Machine Learning Perspective.", Wiley-Blackwell., (2007)..

[10] D. e. a. Inman, ". "Structural Health Monitoring: An Overview."," *Journal of Aerospace Engineering,,* vol. 12, no. 2, pp. 48-55., (2001).

[11] A. Rytter, "Vibration-based Inspection of Civil Engineering Structures." PhD Thesis,, Dept. of Building Technology and Structural Engineering, Aalborg University, 1993).

[12] H. e. a. Sohn, ""Structural Health Monitoring with Data Fusion."," *Structural Health Monitoring, ,* vol. 3, no. (4), , pp. 367-390., (2004)..

[13] K. e. a. Worden, " "Damage Detection in Structures using Statistical and Machine Learning Techniques.",," *Journal of Structural Health Monitoring,* vol. 6, no. (2), pp. , 89-100., (2007)..

[14] L. e. a. Zhang, " "IoT-enabled SHM Systems for Smart Cities."," *Journal of Smart Structures and Systems, ,* Vols. 557-573., no. (4),, p. 23, (2019)..

[15] S. &. R. K. Suresh, " "Acoustic Emission Techniques for Structural Health Monitoring."," *Engineering Fracture Mechanics,,* vol. 52, no. (4), , pp. 571-585., (1995)..

[16] X. e. a. Zhao, " "Temperature Effects on Structural Health Monitoring Systems."," *Structural Health Monitoring, ,* vol. 6, no. (2), , pp. 175-192., (2007)..

[17] C. e. a. Grosse, ""Monitoring of Concrete Structures: Influence of Environmental Conditions." ,," *Smart Materials and Structures,,* vol. 11, no. (5), pp. 800-809., (2002). .

[18] H. e. a. Cui, ""Effects of Environmental Conditions on Sensor Performance in Structural Health Monitoring."," *Sensors and Actuators A: Physical, ,* vol. 144, no. (1),, pp. 165-172., (2008). .

[19] K. e. a. Carper, " "Impact of Corrosion on Structural Health Monitoring Systems."," *Journal of Structural Engineering, ,* vol. 126, no. (3),, pp. 376-384., (2000)..

[20] M. A. C. M. S. &. V. C. Machado, " Embedded Sensors for Structural Health Monitoring: Methodologies and Applications Review.," *Sensors, ,* vol. 22, no. (21) 8320, (2022)..

[21] F. G. W. &. W. K. Yao, ". Piezoelectric Materials and Sensors for Structural Health Monitoring: Fundamental Aspects, Current Status, and Future Perspectives. https://doi.org/10.3390/s23010543," *Sensors, ,* vol. 23, no. (1), p. 543., (2023).

[22] L. S. Y. &. G. V. Yu, ". Piezoelectric Transducer-Based Structural Health Monitoring. https://doi.org/10.3390/s24113438," *Sensors, ,* vol. 24, no. (11), , p. 3438. , (2024).

[23] Y. N. A. M. &. A. A. H. Xie, ". Piezoelectric Sensing Techniques in Structural Health Monitoring: A State-of-the-Art Review. https://doi.org/10.3390/s20133730," *Sensors, ,* vol. 20, no. (13),, p. 3730. , (2020).

[24] S. &. S. C. K. Bhalla, " Structural Impedance-Based Damage Diagnosis by Piezo-Transducers. https://doi.org/10.1002/eqe.378," *Earthquake ,Engineering & Structural Dynamics,* vol. 33, no. (4),, pp. 1021-1042., (2004)..

[25] Z. &. Z. X. Sun, " Advances in Electromechanical Impedance Techniques for Structural Health Monitoring: A Comprehensive Review.," *Journal of Civil Structural Health Monitoring, ,* Vols. 10, , no. https://doi.org/10.1007/s13349-020-00402-w, p. 549–569. , 2020.

[26] V. Giurgiutiu, Structural health monitoring: with piezoelectric wafer active sensors., Elsevier, (2007)..

[27] A. &. C. C. E. S. Raghavan, " Review of Guided-Wave Structural Health Monitoring.," *Shock and Vibration Digest,,* vol. 39, no. (2), , pp. 91-114, (2007)..

[28] Z. Y. L. &. L. Y. Su, ". Guided Lamb Waves for Identification of Damage in Composite Structures: A Review. ,. https://doi.org/10.1016/j.jsv.2006.01.020," *Journal of Sound and Vibration,* vol. 295, no. (3-5),, pp. 753-780, (2006).

[29] X. P. B. S. K. A. &. C. H. L. Qing, ". Smart Layer and Smart Carpet for Structural Health Monitoring of Composite Structures.," *Smart Materials and Structures, ,* vol. 4332, (2001).

[30] S. a. K. S. C. Bhalla, " Structural impedance based damage diagnosis by piezo-transducers.., https://doi.org/10.1002/eqe.307," *Earthquake Engng. Struct. Dyn,* vol. 32: , pp. 1897-1916., (2003),.

[31] E. K.-J. X. Y. M. N. A. A. A. Jiao P, " Piezoelectric Sensing Techniques in Structural Health Monitoring: A State-of-the-Art Review. https://doi.org/10.3390/s20133730," *Sensors. ,* vol. 20, no. (13), p. :3730. , 2020;.

[32] G. C. H. H. &. I. D. J. Park, ". An Integrated Health Monitoring Technique Using Structural Impedance Sensors.," *Journal of Intelligent Material Systems and Structures,,* vol. 11, no. (6), , pp. 448-455. , (2000).

[33] S.-X. C. Y.-Q. N. a. A. W.-H. C. Lu Zhou, "a hybrid model for real-time monitoring of multiple bolt looseness using electromechanical impedance and graph convolutional networks," *Smart Materials and Structures,* vol. 30, no. 3, 2021.

[34] V. Giurgiutiu, " "Piezoelectric Wafer Active Sensors for Structural Health Monitoring of Composite Structures Using Tuned Guided Waves.","* ASME. J. Eng. Mater. Technol. ,* vol. 133 , no. (4):, p. 041012., (October 20, 2011)..

[35] G. C. H. a. I. D. Park, ", Feasibility of using impedance-based damage assessment for pipeline structures.,," *Earthquake Engng. Struct. Dyn.,* vol. 30: , pp. 1463-1474., (2001).

[36] Y. Y. A. S. K. N. Y. L. C. K. S. Chin-Wee Ong, " "Application of the electromechanical impedance method for the identification of in-situ stress in structures," ,," *Proc. SPIE, Smart Structures, Devices, and Systems,* vol. 4935, 14 November 2002.

[37] S. a. K. S. C. Bhalla, " Structural impedance based damage diagnosis by piezo-transducers," *. Earthquake Engng. Struct. Dyn., ,* vol. 32: , pp. 1897-1916., (2003),.

[38] S. C. Bhalla S, ". Electromechanical Impedance Modeling for Adhesively Bonded Piezo-Transducers.," *Journal of Intelligent Material Systems and Structures.,* vol. 15, no. 12, pp. 955-972., 2004;.

[39] L. W. Kevin K. Tseng, "Structural damage identification for thin plates using smart piezoelectric transducers,," *Computer Methods in Applied Mechanics and Engineering,,* Vols. 194,, no. 27–29, pp. 3192-3209, 2005.

[40] C. &. V. M. Providakis, "Damage Detection Using Electromechanical Impedance Signatures and statistical outliers.," (2006). .

[41] Y. &. H. Y. Yang, " Electromechanical impedance modeling of PZT transducers for health monitoring of cylindrical shell structures.," *Smart Materials and Structures. 17. 015005. 10.1088/0964-1726/17/01/015005. ,* vol. 17, (2007)..

[42] S. Y. C.-..-B. a. I. D. PARK, ", Structural health monitoring using electro-mechanical impedance sensors.," *Fatigue & Fracture of Engineering Materials & Structures,,* vol. 31: , pp. 714-724., (2008).

[43] P. R. Venu Gopal Madhav Annamdas, " "Influence of the excitation frequency in the electromechanical impedance method for SHM applications,"," *Proc. SPIE Smart Sensor Phenomena, Technology, Networks, and Systems ,* Vols. 7293,, (7 April 2009).

[44] A. M. a. T. U. M Rosiek, "Uncertainty and sensitivity analysis of electro-mechanical impedance based SHM system," in *IOP Conference Series: Materials Science and Engineering, Volume 10, 9th World Congress on Computational Mechanics and 4th Asian Pacific Congress on Computational Mechanics*, Sydney, Australia, 19–23 July, 2010, .

[45] T. B. S. &. B. B. Visalakshi, "Detection and quantification of corrosion using electro-mechanical impedance (EMI) technique.," *International Journal of Earth Sciences and Engineering,,* vol. 4, no. (6), , pp. 889-891., (2011)..

[46] F. G. F. J. V. & I. D. J. Baptista, ". Real-time multi-sensors measurement system with temperature effects compensation for impedance-based structural health monitoring.," *Structural Health Monitoring, ,* vol. 11, no. (2),, pp. 173-186., (2012).

[47] M. L. T. Siebel, ""Experimental Investigation on Improving Electromechanical Impedance-based Damage Detection by Temperature Compensation https://doi.org/10.4028/www.scientific.net/KEM.569-570.1132,"," *Key Engineering Materials, ,* Vols. . 569-570, , July 2013..

[48] D. E. B. V. A. D. d. A. a. J. A. C. U. Fabricio G. Baptista *, " "An Experimental Study on the Effect of Temperature on Piezoelectric Sensors for Impedance-Based Structural Health Monitoring doi:10.3390/s140101208,"," *MDPI,* pp. 1208-1227,, 2014..

[49] R. F. B. N. M. L. M. E. M. V, ", "Structural health monitoring in composites based on probabilistic reconstruction techniques. https://doi.org/10.1016/j..2016..,"," *proeng,* vol. 11., no. 668, pp. 48-55, , 2016. .

[50] C. P. a. M. T. Victor Giurgiutiu, " "Radiation, temperature, and vacuum effects on piezoelectric wafer active sensors DOI 10.1088/0964-1726/25/3/035024,"," *IOP Science, ,* Feburary 2016..

[51] C. H. N. G. M. R. N. M. C. B. E. LIZE, ", "Combination of frequency shift and impedance-based method for robust temperature sensing using piezoceramic devices for shm ⟨hal-01620039⟩,"," in *in EWSHM* , Bilbao, Spain.,, 2016..

[52] T. R. a. N. K. M. Alamdari, ", "A spectral-based clustering for structural health monitoring of the Sydney Harbour Bridge,"," *Mechanical Systems and Signal Processing, ,* pp. 384-400, , 2017. .

[53] M. A. V. F. J. De Oliveira MA, " A New Structural Health Monitoring Strategy Based on PZT Sensors and Convolutional Neural Network.," *Sensors.,* vol. 18, no. (9):, p. 2955. , 2018;.

[54] C. N. G. B. V. F. J. Antunes RA, " Modeling, Simulation, Experimentation, and Compensation of Temperature Effect in Impedance-Based SHM Systems Applied to Steel Pipes. https://doi.org/10.3390/s19122802," *Sensors.,* vol. 19, no. (12):, p. 2802., 2019; .

[55] J. d. R. V. d. M. J. R. M. F. N. C. A. G. a. V. S. Stanley Washington Ferreira de Rezende1, Convolutional neural network and impedance-based SHM applied to damage detection, IOP Publishing ltd, 11 September 2020.

[56] F. &. K. Z. S. Lambinet, "Damage detection & localization on composite patch repair under different environmental effects.," *Engineering Research Express, ,* vol. 2, no. 4, p. 045032, (2020)..

[57] T. J. Gayakwad H, "Structural Damage Detection through EMI and Wave Propagation Techniques Using Embedded PZT Smart Sensing Units. https://doi.org/10.3390/s22062296," *Sensors. ,* vol. 22, no. (6):, p. 2296., 2022; .

[58] I. K. George M. Sapidis, " "A Deep Learning Approach for Autonomous Compression Damage Identification in Fiber-Reinforced Concrete Using Piezoelectric Lead Zirconate Titanate Transducers https://doi.org/10.3390/s24020386,"," *MDPI, ,* 9 January 2024..

[59] C. R. &. W. K. Farrar, Structural health monitoring: a machine learning perspective., John Wiley & Sons., (2012). .